HAL
open science

Thermal model of water and CO activity of comet C/1995 O1 (Hale-Bopp)

N. Gortsas, Ekkehard Kührt, U. Motschmann, H.U. Keller

To cite this version:

N. Gortsas, Ekkehard Kührt, U. Motschmann, H.U. Keller. Thermal model of water and CO activity of comet C/1995 O1 (Hale-Bopp). Icarus, 2011, 212 (2), pp.858. 10.1016/j.icarus.2011.01.017 . hal-00734587

HAL Id: hal-00734587

https://hal.science/hal-00734587v1

Submitted on 24 Sep 2012

HAL is a multi-disciplinary open access archive for the deposit and dissemination of scientific research documents, whether they are published or not. The documents may come from teaching and research institutions in France or abroad, or from public or private research centers.

L'archive ouverte pluridisciplinaire **HAL**, est destinée au dépôt et à la diffusion de documents scientifiques de niveau recherche, publiés ou non, émanant des établissements d'enseignement et de recherche français ou étrangers, des laboratoires publics ou privés.

Accepted Manuscript

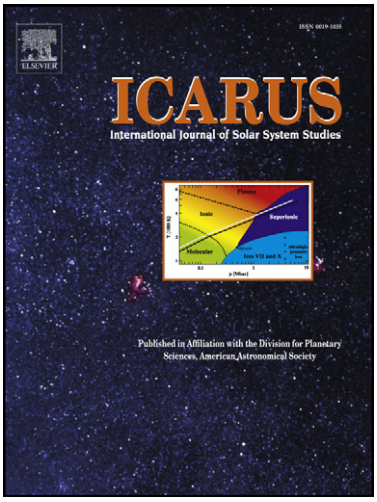

Thermal model of water and CO activity of comet C/1995 O1 (Hale-Bopp)

N. Gortsas, E. Kührt, U. Motschmann, H.U. Keller

PII: S0019-1035(11)00028-5
DOI: 10.1016/j.icarus.2011.01.017
Reference: YICAR 9696

To appear in: *Icarus*

Received Date: 7 March 2010
Revised Date: 9 January 2011
Accepted Date: 14 January 2011

Please cite this article as: Gortsas, N., Kührt, E., Motschmann, U., Keller, H.U., Thermal model of water and CO activity of comet C/1995 O1 (Hale-Bopp), *Icarus* (2011), doi: 10.1016/j.icarus.2011.01.017

This is a PDF file of an unedited manuscript that has been accepted for publication. As a service to our customers we are providing this early version of the manuscript. The manuscript will undergo copyediting, typesetting, and review of the resulting proof before it is published in its final form. Please note that during the production process errors may be discovered which could affect the content, and all legal disclaimers that apply to the journal pertain.

ACCEPTED MANUSCRIPT

Thermal model of water and CO activity of comet C/1995 O1 (Hale-Bopp)

N. Gortsas[a,e], E. Kührt[b,e], U. Motschmann[c,e,f], H. U. Keller[d,g]

[a]*Phone: +49 30 67055 461, Fax: +49 30 67055 386, Email: Nikolaos.Gortsas@dlr.de*
[b]*Phone: +49 30 67055 514, Fax: +49 30 67055 386, Email: Ekkehard.Kuehrt@dlr.de*
[c]*Phone: +49 531 391 5186, Fax: +49 531 391 5833, Email: Uwe.Motschmann@tu-bs.de*
[d]*Phone: t.b.a, Fax: t.b.a, Email: keller@linmpi.mpg.de*
[e]*Institute of Planetary Research, German Aerospace Center, Rutherford Str. 2, D-12489 Berlin, Germany*
[f]*Institute of Theoretical Physics, Technical University of Braunschweig, Mendelssohnstr. 3, D-38106 Braunschweig, Germany*
[g]*Institute for Geophysics and Extraterrestrial Physics, Technical University of Braunschweig, Mendelssohnstr. 3, D-38106 Braunschweig, Germany*

Abstract

An investigation of the activity of comet C/1995 O1 (Hale-Bopp) with a thermophysical nucleus model that does not rely on the existence of amorphous ice is presented. Our approach incorporates recent observations allowing to constrain important parameters that control cometary activity. The model accounts for heat conduction, heat advection, gas diffusion, sublimation, and condensation in a porous ice-dust matrix with moving boundaries. Erosion due to surface sublimation of water ice leads to a moving boundary. The movement of the boundary is modeled by applying a temperature remapping technique which allows us to account for the loss in the internal energy of the eroded surface material. These kind of problems are commonly referred to as Stefan problems. The model takes into account the diurnal rotation of the nucleus and seasonal effects due to the strong obliquity of Hale-Bopp as reported by Jorda et al. [1997]. Only bulk sublimation of water and

ACCEPTED MANUSCRIPT

CO ice *needs to be* **are** considered without further assumptions *like* **such as** amorphous ices with certain amount of occluded CO gas. Confined and localized activity patterns are investigated following the reports of Lederer and Campins [2002] about the chemical heterogeneity of Hale-Bopp and of Bockelée-Morvan et al. [2009] about a strong CO source at a latitude of 20°. The best fit to the observations of Biver et al. [2002] is obtained with a low thermal conductivity of 0.01 W m^{-1} K^{-1}. This is in *good* agreement with recent results of the Deep Impact mission to 9P/Tempel 1 [Groussin et al., 2007] and with previous thermal simulations [Kührt , 1999]. *The water production curve matches the water production rates of Biver et al. [2002] well.* **The water production curve matches the production rates well from -4AU pre-perihelion to the outgoing leg while the model does not reproduce so well the water production beyond 4AU pre-perihelion.** The CO production curve *fits remarkably well the CO* **is a good fit to the** measurements of Biver et al. [2002] over the whole measured heliocentric range from -7AU pre- to 15AU post-perihelion.

Key words: Comet Hale-Bopp, Comets, Nucleus, Comets, Composition, Thermal histories, Comets, Origin, Comets, Coma

---

1. Introduction

The long period comet C/1995 O1 (Hale-Bopp) was discovered in July 1995 at a heliocentric distance of 7.2AU. Its **high** intrinsic brightness already at 7AU offered the unique opportunity to study the evolution of cometary activity over a wide range of heliocentric distances pre- and post-perihelion. The obtained data set of production rates contains important information

ACCEPTED MANUSCRIPT

about the physical and chemical state of the nucleus. Thermophysical nucleus models provide a *mean* **means** to access this information by matching calculated production rates to those derived from observations. In particular, measurements of the nuclear activity over a wide range of heliocentric distances pre- and post-perihelion strongly constrain the model assumptions and parameters. Near the Sun the absorbed energy is mainly used to maintain cometary activity while at larger heliocentric distances when the activity subsides the fractions of energy going *for* **to** re-radiation and transfer into the nucleus interior become dominant.

Comet Hale-Bopp has been studied *by* **with** a wide range of instruments. A good overview of the employed techniques and a discussion of the early understanding of the observations can be found in Bockelée-Morvan and Rickman [1997]. From ground-based radio telescopes production rates for a variety of species were derived. A progressive release pattern for species like CO, CH_3OH, HCN, H_2O (from OH) and many others along the incoming branch has been detected [Jewitt et al., 1996; Biver et al., 1997]. In addition, water production rates have been contributed by other groups [Colom et al. , 1997; Stern et al. , 1999; Weaver et al. , 1999; Crovisier et al. , 1999]. Biver et al. [2002] updated their observations twice summarizing in their 2002 publication the full set of observations covering a heliocentric distance from -7AU pre- to 15AU post-perihelion.

Among the first who studied comet Hale-Bopp with a thermal model was Prialnik [1997a]. The model assumed that 5% of CO gas is occluded in an amorphous ice matrix. The calculated CO curve **after perihelion** is *after perihelion* almost constant in contradiction with CO observations. A similar

ACCEPTED MANUSCRIPT

result was reported by Flammer et al. [1998] who also obtained an almost flat CO curve. *In this model is* **Their model** assumed that there are H_2O clathrate grains with occluded CO gas. However, the observations of Jewitt et al. [1996] and Biver et al. [1997] show a peak in CO production around perihelion. Later, Prialnik [1997b] presented a thermal model to study the long**-term** *distance* evolution of Hale-Bopp. A key model assumption is the existence of *an amorphous ice matrix* **amorphous water ice** with occluded CO gas. But the model does not resolve the diurnal rotation of the comet. At that time, only few pre-perihelion observations were available.

Enzian et al. [1998] presented a thermal model of Hale-Bopp and compared their results for water and CO with pre-perihelion observations. Key model assumptions are the existence of amorphous ice with occluded CO gas. A modest fit *through* **to** the available data points of CO *has been* **was** achieved by assuming 10% of CO occluded in amorphous ice, 0° obliquity of the rotation axis, and an argument of the sub-solar meridian of 0°. The water observations could not be fitted prior to 4AU pre-perihelion. An estimate of the possible contribution of an extended water source due to water ice sublimation from icy grains in the coma is given. The proposed estimate allows to fit the data points beyond 4AU. On the post-perihelion branch, however, it is apparent that the water contribution of the extended source exceeds the observations. When the data set of Biver et al. [1997] became available, Enzian [1999] applied again his thermal model on Hale-Bopp. He considered two different values of the obliquity of the rotation axis 0° and 90°. The chemical composition of the comet was made up with 50% mass of dust, 40% amorphous water ice, 5% CO trapped in amorphous water ice,

ACCEPTED MANUSCRIPT

and 5% CO ice as an independent phase. With these assumptions the author was able to reproduce the pre-perihelion CO outgassing pattern with an obliquity of 90°. The fit of the CO data along the post-perihelion branch is modest and ends at 4AU post-perihelion. The data fit with 0° obliquity of the rotation axis was poor pre- and post-perihelion. At the same time, the water production rates could not be fitted beyond 4AU pre-perihelion.

Kührt [1999] showed that a thermophysical nucleus model is able to match the water sublimation measurements without the assumption of extended water sources in the coma. Based on the strong obliquity of Hale-Bopp as reported by Jorda et al. [1997], Kührt [1999] investigated the apparent**ly** strong influence of seasonal effects on the water sublimation curve. He showed that it is possible to fit the water production rates if a low thermal conductivity is used.

Capria et al. [2000] published a thermal model of comet Hale-Bopp and compared their results with CO observations in the range from -7AU pre- to 3AU post-perihelion. The best fit to the data set which was available at that time was achieved by assuming that CO exists as an independent ice phase and that 20% of the CO is released only after water sublimation. Another 10% of the CO gas is trapped in amorphous ice. *No water sublimation curves are shown in this paper.* In a later article, Capria et al. [2002] compared their results for the water and CO activity of Hale-Bopp with observations in the range from -7AU pre- to 4AU post-perihelion. The calculated water flux fits the observations only in the range from -2AU to -1AU, pre-perihelion. The remaining data points in the range from -5AU to -2AU are not fitted by the model, neither are the data points along the post-perihelion branch. The

ACCEPTED MANUSCRIPT

assumptions of the trapped CO ice are similar to those of Capria et al. [2000]. *While the fit is similar to Capria et al. [2000] good in the range from -2AU to -1AU the curve is an upper limit to the observations in the range from -7AU to -2AU.* **In the range from -2AU to -1AU the fit to the CO data is good as in Capria et al. [2000]. In the range from -7AU to -2AU the curve is an upper limit to the observations.** The same holds for the post-perihelion branch. The range covered along the post-perihelion branch is 1AU to 4AU. The curve does not match the data points so well.

It can be concluded that the model**s** of Enzian [1999] and Capria et al. [2002] *seem to* fit the observations of Hale-Bopp for CO *quite well although both models have not been applied* **quite well although neither model has been applied** to the full data set covering a range from -7AU pre- to 15AU post-perihelion as reported by Biver et al. [2002]. Both models employ similar assumptions on the existence of amorphous ice and the amount of occluded CO gas (5 to 20%). The water production curve could not be reproduced *so well by either of them* **so well by either model**. Both suggest that extended sources might be responsible for the water sublimation beyond 4AU pre-perihelion.

In this article, a thermal model is presented and applied to comet Hale-Bopp which relies only on the assumption of CO ice bulk sublimation and on seasonal effects. Confined and localized activity of water and CO ice is studied following recent observational evidence*s* on important properties of comets [Lederer and Campins, 2002; Groussin et al., 2007; Bockelée-Morvan et al., 2009] and earlier results of Kührt [1999] on the importance of seasonal effects and a low thermal conductivity. *There is no need to include*

ACCEPTED MANUSCRIPT

amorphous ice for which no observational evidence has been found in the Solar System [Huebner , 2009]. **Amorphous ice is not included in the model calculations. Its existence in comets is still under discussion [Huebner , 2009].** The model solves the heat and mass transfer problem for cometary activity with a sophisticated method to deal with moving boundaries. Heat conduction, heat advection, gas diffusion, sublimation and condensation are taken into account. The movement of the surface boundary is implemented following the concept of Crank and Gupta [1972]. This kind of moving boundary problems are referred to as Stefan problems [Crank , 1984]. The model is applied to the full data set of water and CO production rates covering a range from -7AU pre- to 15AU post-perihelion as reported by Biver et al. [2002].

The article is organized as follows: in the next section we briefly introduce the thermal model. Then a brief collection on recent observational findings of important parameters follows. We then present our simulations based on these observations. At the end, conclusions are drawn. **The article is organized as follows: The thermal model is introduced in Section 2. A collection of recent observational findings are given at the beginning of Section 3. The simulation results follow this discussion. In Section 4 conclusions are drawn.**

2. Model description

2.1. Thermal model

Our model comet consists of water ice, CO ice, dust and pores. Further components can principally be added. The model solves the coupled heat

ACCEPTED MANUSCRIPT

and mass transfer problem with moving boundary conditions.

In a volume element energy is transported through heat conduction of the ice matrix, heat advection of the vapor, and sublimation or condensation processes in the pores. A theoretical description of these processes starts with the general formulation of the conservation laws of mass, momentum, and energy as appropriate for comets. Mass conservation is expressed through a balance equation for the vapor mass density ρ_μ and the solid ice mass density ρ_μ^s of species μ

$$\frac{\partial \rho_\mu}{\partial t} + \nabla(\rho_\mu u_\mu) = -\frac{\partial \rho_\mu^s}{\partial t}, \tag{1}$$

and

$$\frac{\partial \rho_\mu^s}{\partial t} = -q_\mu \,. \tag{2}$$

x and t denote the spatial and temporal coordinates. u_μ denotes the **diffusion** velocity of the μ volatile component. The source term q_μ defines bulk evaporation. Following Mekler et al. [1990] it can be calculated as the difference between the gas density ρ_μ of species μ in the pores and the equilibrium state $\rho_{\mu,eq}$ at some bulk temperature T

$$q_\mu = f_p \left(\rho_{\mu,eq} - \rho_\mu\right) c_{th,\mu}(T) \,. \tag{3}$$

Here $c_{th,\mu}$ denotes the **mean** thermal velocity of the μ gas species and f_p is a factor that depends on structural properties of the comet, e.g. $f_p = 2\,\psi/r_p$ with ψ being the porosity and r_p the effective pore radius. In this model the pores are modeled as cylindrical capillaries whose circular cross-section has a diameter of $2\,r_p$ [Mekler et al., 1990]. The $\rho_{\mu,eq}$ is given by the vapor pressure which is calculated with the Clausius-Clapeyron equation and the

ACCEPTED MANUSCRIPT

assumption that the gas obeys the ideal gas law

$$\rho_{\mu,eq} = \frac{P_{v,\mu}\, m_\mu}{k_B\, T}\,. \tag{4}$$

m_μ and k_B denote the mass of species μ and the Boltzmann constant, respectively. The saturation pressure $P_{v,\mu}$ is given according to the empirical formula of Fanale and Salvail [1984] as $P_{v,\mu}(T) = A_\mu \exp(-B_\mu/T)$. The values of the constants can be found in Table 1. An implicit assumption of this approach is that there is bulk ice in the pores so that the reference state can prevail. *If there is no bulk ice and if the thermodynamic conditions prevent condensation, then the source term is zero.*

The mean free path of molecules exceeds the characteristic length scale of a porous nucleus, e.g. the lengths characterizing the structure of the pores. Therefore, the Knudsen number is much larger then 1. In this case the vapor velocity field can be calculated from the Knudsen formula

$$\rho_\mu u_\mu = -C_\mu \frac{\partial}{\partial x}(\rho_\mu \sqrt{T})\,. \tag{5}$$

C_μ is a factor that can be related to structural and thermal parameters [Benkhoff and Spohn, 1991], e.g. $C_\mu = 2\,\psi\, r_p\, c_{th,\mu}$.

Equation (1) and (5) describe the diffusion of vapor inside a predefined porous structure in a macroscopic model. The conservation of energy written in terms of temperature under the assumptions of a Fourier type heat flux, the advection of energy through vapor flow, and an energy source term reads as, e.g. Spohn and Benkhoff [1990],

$$c\,\rho\,\frac{\partial T}{\partial t} + \sum_\mu c_{g,\mu}\,\rho_\mu\, u_\mu \frac{\partial T}{\partial x} = \frac{\partial}{\partial x}\kappa\frac{\partial T}{\partial x} - \sum_\mu \Delta H_\mu q_\mu\,. \tag{6}$$

ACCEPTED MANUSCRIPT

$c_{g,\mu}$ denotes the specific heat of vapor of species μ. It is calculated by assuming the validity of the ideal gas law for water and CO vapor. Dust enters the model via $c\rho = \sum_\mu c_\mu, \varrho_\mu$. ϱ_μ **denotes the bulk density of species** μ **which equals** $\varrho_{b,\mu}\,\gamma_\mu$**.** $\varrho_{b,\mu}$ **and** γ_μ **denote the solid bulk velocity and the volumetric filling factor of species** μ**.** The sum goes over all constituents of the material, e.g. solid and vapor. It reduces the active surface fraction with respect to pure porous ice [Davidsson and Skorov , 2002b].

The description is one dimensional with respect to the processes taking place inside the nucleus. But the boundary condition accounts for different irradiation patterns which allows us to consider active surface areas throughout the comet surface. The one dimensional description is justified because the lateral components of the thermal conduction coefficient are assumed to be small compared to the radial direction, see also the discussion below on the thermal conduction coefficient. In addition, processes related to cometary activity are believed to be confined in the range of few cm to meters. This is small compared to the radius of a comet of several km size. Therefore, it is safe to employ the plane parallel approximation.

Energy transport through heat conduction in the ice matrix is described by the first term on the right hand side of Eq. (6). Its contribution to the energy budget *heavily depends* **depends heavily** on the choice of the thermal conduction coefficient κ which describes energy transport in the solid phase (grains and ices). It depends on the structure and composition of cometary material and it is sometimes assumed to be temperature dependent. Some authors also include radiative heat transfer to κ but at temperatures typical for comets it can be neglected. Steiner and Kömle [1991] presented

ACCEPTED MANUSCRIPT

an approach to add the heat transport by vapor flux through the pores to the thermal conduction coefficient κ.

On the experimental side, there are studies of the thermal conductivity of porous ice in connection with comets. For a review on various measurements, especially for water ice phases, consult Seiferlin et al. [1996] and Seiferlin [1991] and the bibliography therein.

However, many unsolved questions like the existence of amorphous ice or the porosity and pore size distribution in cometary nuclei make it difficult to derive realistic values. Laboratory measurements [Spohn et al. , 1989; Seiferlin , 1991; Grün et al., 1993; Stöffler et al., 1991] generally suffer from the widely unknown structure and composition of cometary matter and may not be representative. We, therefore, developed a model that tries to keep the number of free parameters as low as possible by incorporating what is currently known based on recent observations of and missions to comets [Jorda et al., 1997; Fernández , 2002; Lederer and Campins, 2002; Groussin et al., 2007; Bockelée-Morvan et al., 2009].

2.2. Characteristic time scales

We perform a thorough analysis of the relevant time scales to evaluate the importance of the terms in Eq. (1) [Spohn and Benkhoff, 1990]. The analysis is carried out for water vapor but is equally applicable to CO vapor. We therefore drop the μ index. The characteristic time scales of heat conduction τ_h and gas diffusion τ_g can be expressed as

$$\tau_h = \frac{L^2 \rho\, c}{\kappa} \tag{7}$$

ACCEPTED MANUSCRIPT

and τ_g as

$$\tau_g = \frac{L^2}{C\,\sqrt{T}}\,. \tag{8}$$

L denotes a characteristic length scale of the problem. It cannot exceed the mean free path of the vapor molecules because then the flow is deviating from the free molecular flow regime. In case that the pores are modeled to be cylindric tubes L describes the length of the pores while the previously introduced pore radius r_p describes the radius of their cross-section.

All quantities in Eq. (1) are scaled to dimensionless quantities which are indicated by a * superscript. Time is referred to the heat time scale $t^* = t/\tau_h$. x **The depth** x is scaled to L L, e.g. $x^* = x/L$. The vapor density is scaled to an equilibrium value at the surface temperature of a water **ice** covered **nucleus** *comet* at perihelion $\rho^* = \rho/\rho_{eq}$. The velocity field is scaled to the thermal velocity at the surface temperature at perihelion, e.g. $u^* = u/c_{th}$. The mass source term which describes the change of vapor density with time is scaled to the ratio of the vapor density reference value ρ_{eq} and the time scale of gas diffusion τ_g, e.g. $q^* = q\,\tau_g/\rho_{eq}$. Mapping of Eq. (1) to dimensionless quantities leads then to

$$\frac{\tau_g}{\tau_h}\frac{\partial \rho^*}{\partial t^*} + \frac{\tau_g\,c_{th}}{L}\,\frac{\partial(\rho^*\,u^*)}{\partial x^*} = q^*\,. \tag{9}$$

Entering the expressions of the characteristic scales leads to

$$\frac{\kappa}{\rho\,c\,2\psi\,c_{th}}\frac{1}{r_p}\frac{\partial \rho^*}{\partial t^*} + \frac{1}{2\psi}\sqrt{\frac{L^3}{r_p^3}}\,\frac{\partial(\rho^*\,u^*)}{\partial x^*} = q^*\,. \tag{10}$$

The coefficient of the time derivative is only **significant** for very small pore radii, e.g. $r_p < 10^{-8}$m, in the same range as the second term on the left hand side of the equation. For typical pore sizes of comets in the range of **a**

ACCEPTED MANUSCRIPT

few to 100 μm it is thus safe to neglect the temporal variations of the vapor density. We therefore solve the mass conservation equation Eq. (1) without the temporal variation of the mass density yielding

$$\nabla(\rho_\mu u_\mu) = q_\mu \,. \tag{11}$$

The obtained set of coupled equations is then solved numerically on a grid that is modified according to the techniques discussed below.

2.3. Boundary conditions

The heat transfer equation is closed by appropriate boundary conditions. At the surface the energy balance equation in Wm^{-2} provides a commonly used boundary condition which is only very briefly discussed here

$$\begin{aligned} \frac{F_{S,0}}{r_H^2(t)} \left(\quad 1 \quad -\mathcal{A} \right) \max_{\zeta\in[0,2\pi)} \{0, \cos(\zeta)\} &= \epsilon_{em}\, \sigma T^4 \\ + \quad \kappa\, \nabla T(x,t) + Q(T) + \sum_\mu c_{g,\mu} \rho_\mu\, u_\mu T \,. \end{aligned} \tag{12}$$

The left hand side of the equation describes the solar irradiation of the surface at some heliocentric distance r_H. $F_{S,0}$ is the solar constant, $\mathcal{A}$ the *bond* **Bond** albedo, and ζ the solar zenith distance. ϵ_{em} and σ are the thermal emissivity and the Stefan-Boltzmann constant, respectively. The angle ζ is important since it controls how the incoming solar energy is distributed over the surface of the nucleus. It is calculated according to the following formulas [Sekanina , 1979]

$$\cos(\zeta) = \cos(\theta)\cos(\phi)\cos(\theta_s) + \sin(\theta)\sin(\theta_s) \tag{13}$$

θ is the latitude, ϕ the hour angle and θ_s the cometocentric latitude of the subsolar point. θ_s is given by

$$\sin(\theta_s) = \sin(\delta)\sin(\Phi + \alpha) \,. \tag{14}$$

ACCEPTED MANUSCRIPT

δ is the obliquity and Φ the argument of the sub-solar meridian at perihelion. The true anomaly α of the comet is calculated by using Kepler's equations. The terms *of* **on** the right hand side of Eq. (21) describe surface reemission due to the Stefan-Boltzmann law, thermal conduction between the surface and the nucleus, surface ice sublimation, and energy transport from the gas phase. In our model the nucleus surface is covered by water ice of volume fraction f_i and dust. The orientation of our coordinate system is such that $x = 0$ denotes the surface of the nucleus and $x = x_b$ the bottom. The surface sublimation term is given by the Hertz-Knudsen formula

$$Q_\mu(T) = f_\mu \, \Delta H_\mu \, P_{v,\mu}(T) \sqrt{\frac{m_\mu}{2\pi \, k_B T}} \, . \tag{15}$$

The lower boundary is given by the constraint that the thermal flux vanishes

$$\kappa \, \nabla \, T(x_b, t) = 0 \, . \tag{16}$$

This adiabatic approach expresses the assumption that a quasi-stationary state is reached in a rotating body at depths beyond *some***many diurnal** skin depths of the thermal wave. Depending on the value of the thermal conductivity the position of the lower boundary has been chosen to secure a vanishing thermal flux well above the lower boundary.

A boundary condition for the gas diffusion problem is difficult to obtain, see e.g. the discussion in Skorov et al. [2001] and Davidsson and Skorov [2004]. At this stage, we follow the approach of most groups and set the vapor density equal to zero at the surface for CO, see e.g. Mekler et al. [1990]

$$\rho_{co}(x = 0) = 0 \, . \tag{17}$$

ACCEPTED MANUSCRIPT

For water vapor we follow Spohn and Benkhoff [1990] and set its value to the equilibrium conditions at the given surface temperature T_s

$$\rho_v(x=0) = \rho_{v,eq}(T_s)\,. \tag{18}$$

2.4. Stefan problem of comets

The thermal evolution of comets needs to be treated as a Stefan problem if the thermal conductivity is low (< 0.1 W m^{-1}K^{-1}). In this case, the propagation velocity of the diurnal heat wave

$$v_p = \sqrt{\frac{4\pi\,\kappa}{\rho\,c\,\tau_r}} \tag{19}$$

is comparable to the erosion velocity of surface material $v_e = Q/(\Delta H\,\rho_i)$ at perihelion. τ_r is the diurnal rotation period. Taking typical values for water ice at perihelion shows that both velocities are of the same order, e.g. $\approx 6 \times 10^{-7}$m/s. Hence, the penetration of the nucleus by the diurnal heat wave is obstructed. This effect needs to be resolved by treating the thermal evolution as a Stefan problem.

The set of equations presented in the previous section, i.e. Eq. (1), Eq. (5), and Eq. (6) and its boundary conditions, has to be extended in order to incorporate surface erosion into the model. Due to sublimation of water ice a certain amount of surface material is ejected into space. Hence, the upper boundary is moving as sketched in Fig. 1. This movement poses a challenge to numerical modeling especially to the calculation of the thermal gradient in Eq. (21). In general, the thickness of the eroded surface layer Δs deviates from the spatial discretization size Δx. As a result the distance between the actual location of the surface boundary and the next grid node is less

ACCEPTED MANUSCRIPT

than Δx. In finite-difference schemes there are several approaches to deal with this situation [Crank , 1984]. Our approach is motivated by the work of Crank and Gupta [1972]. The thickness of the eroded surface layer Δs_μ of species μ is obtained from the so called Stefan condition [Stefan , 1891]

$$\frac{\Delta s_\mu}{\Delta t} = \frac{Q_\mu(T)}{\Delta H_\mu \, \rho_\mu} \, . \tag{20}$$

The spatial grid Γ is moved according to this erosion size Δs at each time step, see Fig. 2. The temperature field is obtained at the new grid Γ^* through interpolation by cubic splines. The cubic splines $S_j(x)$, with j counting the number of intervals in the old grid Γ, are given by

$$\begin{aligned} S_j(x) &= s_{j,0} + s_{j,1}\,(x - x_j) + s_{j,2}\,(x - x_j)^2 \\ &+ s_{j,3}\,(x - x_j)^3 \, . \end{aligned} \tag{21}$$

The coefficients $s_{j,*}$ are obtained from a set of continuity conditions up to second order taken at the cell boundaries. x_j denotes the coordinate of the left sided edge of the interval j. Once the cubic spline functions are known the temperature at the new grid Γ^* is obtained through

$$T(x_j^*, t) := S_j(x_j + \Delta s, t) \, . \tag{22}$$

The adaptation of the spatial grid will be called temperature remapping. At each time step the erosion of surface material is taken into account. It is introduced to ascertain a constant spatial discretization despite surface erosion. It is designed to secure that the upper boundary is located on a grid node at each time step. Besides loss of energy through surface sublimation and thermal emission the nucleus is also losing the internal energy of the eroded surface material.

ACCEPTED MANUSCRIPT

The mass and flux densities are only linearly interpolated to the new grid. Numerical calculations have shown that for the gas density a higher accuracy is not as important as for the temperature which controls the amount of energy entering the nucleus. This approach also reduces the amount of computing time considerably.

2.5. Grid adaptation

In comets sublimation does not only occur at the surface but also in the interior. In this article an additional volatile species subliming from the interior is considered, e.g. CO. While the situation at the surface remains as in the previous subsection, the fact that there is a volatile species in the interior leads to a moving material interface. Therefore, the depth of the CO front denoted by Λ_{co} is time dependent. The number of grid nodes $N_\Lambda(t)$ distributed over Λ_{co} is obtained from

$$N_\Lambda(t) = \frac{\Lambda_{co}(t)}{\Delta x}\,. \tag{23}$$

Δx is the spatial discretization size, which is kept constant throughout the computation. Initially, the material interface is located on a grid node which means that $N_\Lambda(t)$ is an element of $\mathbf{N}$, the set of all positive integers,

$$N_\Lambda(t) \in \mathbf{N}\,. \tag{24}$$

In general, CO sublimation leads to a violation of condition Eq. (24). This movement of the CO front is resolved by first solving Eq. (20) for CO. Second, the amount of surface erosion $\Delta s_i(t)$ and the movement of the CO front $\Delta s_{co}(t)$ is collected for several time steps, e.g. $t_1, ..., t_N$,

$$\Lambda_{co}(t_N) = \sum_{j=1}^{N}\Big(\Lambda_{co}(t_{j-1}) + \Delta s_{co}(t_j) - \Delta s_i(t_j)\Big)\,. \tag{25}$$

ACCEPTED MANUSCRIPT

Once the CO front $\Lambda_{co}(t)$ exceeds a grid node from the surface away, the number of grid nodes distributed along $\Lambda_{co}(t)$ is increased by 1. In the opposite case, the CO front $\Lambda_{co}(t)$ exceeds a grid node towards the surface leading to a reduction of the grid nodes distributed over Λ_{co} by 1. Depending whether surface erosion or CO sublimation dominates, the number of grid points between the surface and the CO front will decrease or increase with time. This approach has the benefit to be robust but it does not resolve the actual location of the inner front below the spatial discretization size Δx. It assumes that the CO front remains all the time on a grid node as long as the number of grid nodes does not change according to the described method. This approach is checked against variations of the spatial discretization size and it fulfills the appropriate stability conditions.

2.6. Summary of model assumptions

Based on the arguments given above and on additional numerical studies we start from the following **list of** assumptions **(which is not exhaustive)**:

- *We consider active areas without permanent dust mantles.*
- The heat conductivity of cometary matter is low and, therefore, a careful treatment of the thermal evolution of the comet as a Stefan problem is important.
- Heat conduction, heat advection, gas diffusion, sublimation, and condensation processes are considered.
- *There is no need to include amorphous ice in the model for which no observational evidence has been found in the Solar System [Huebner*

ACCEPTED MANUSCRIPT

, 2009]. **Amorphous ice is not included in the model. Its existence in comets is still under discussion [Huebner , 2009].**

- Dust enters implicitly **into** this model via the material parameters specific heat, density, and thermal conductivity. *The process of dust ejection from the surface is not explicitly modeled because its impact on cometary activity should be small.* **We further assume that all dust grains that are liberated from the ice matrix at the surface are** *driven***carried into the coma by the gas flow, i.e. dust mantle formation is assumed not to take place. Although dust mantle formation appears common among less active comets, the current assumption may be realistic for a highly active comet like Hale-Bopp.**

3. Results

3.1. Calculation setup

The nucleus model of Hale-Bopp assumes a two-layer stratigraphy with the upper layer being a mixture of water ice and dust while the lower layer includes also CO ice. The parameters of the calculations can be found in Table 1, Table 4, and Table 3.

Comet Hale-Bopp is a long period comet with a period of 2500 years. CO and water activity, however, *is determined***occur** when the comet is close to the Sun. Therefore, for this study the comet is put at a heliocentric distance of 20AU and the calculations *are proceeded***proceed from there** to 20AU post-perihelion. This approach was also followed by Enzian et al. [1998] and Enzian [1999].

ACCEPTED MANUSCRIPT

3.2. Observational findings

An important input parameter for the thermal evolution of a comet is the thermal conductivity. Groussin et al. [2007] analyzed the near infrared spectra of the Deep Impact mission to comet 9P/Tempel 1. From these data a low thermal inertia of ≤ 50 W $K^{-1}m^{-2}s^{1/2}$, corresponding to a heat conductivity less than 0.003 W $K^{-1}m^{-1}$, was derived. In addition, Kührt [1999] showed for comet Hale-Bopp that a thermophysical nucleus model with a low thermal conduction coefficient of 0.001 W $K^{-1}m^{-1}$ is able to reproduce the water sublimation measurements by assuming solely water ice sublimation without further assumptions , *like***such as** extended sources [Enzian et al., 1998]. More recently, Davidsson et al. [2009] re-evaluated the infrared spectra of the Deep Impact mission to comet 9P/Tempel 1. They included surface roughness into the model and derived thermal inertia values for most surface areas (inactive surface elements) in the range of 1000 to 3000 W $K^{-1}m^{-2}s^{1/2}$ or about 1 to 10 W $K^{-1}m^{-1}$. Due to the uncertainty of κ we investigated several cases from 0.001 W $K^{-1}m^{-1}$ to 0.1 W $K^{-1}m^{-1}$. The best fit to the observations was obtained with a 0.01 W $K^{-1}m^{-1}$ which is employed for all presented figures of this paper.

The radius of the comet was set to 30 km as reported by Fernández [2002]. Jorda et al. [1997] put the diurnal rotation time of Hale-Bopp to a value of 11.4 h.

Another important input parameter is the obliquity of the rotation axis. The distribution of the incoming solar energy on the surface of the comet heavily depends on this parameter as can be inferred from Eq. (13) and Eq. (14). Following Sekanina [1979], the illumination of a surface area can be

ACCEPTED MANUSCRIPT

calculated if the obliquity and the argument Φ of the sub-solar meridian at perihelion are known. Jorda et al. [1997] published a value for the obliquity of Hale-Bopp of about 84°. This value was used in Kührt [1999] together with an argument Φ of 64° which is slightly below the lower range provided by Vasundhara and Chakraborty [1999]. Enzian et al. [1998] set Φ to 0° which was probably also employed in Enzian [1999]. Vasundhara and Chakraborty [1999] calculated the obliquity and the argument of the sub-solar meridian at perihelion. They published eight values for dates between Oct 6, 1996 to Oct 9, 1997 covering ranges from 77° to 90° for the obliquity and from 68° to 84° for the argument Φ. It seems that these angles are not so well constrained. We, therefore, put the obliquity to a value of 84° which was also published in Jorda et al. [1997] and considered several values for the argument Φ. It turned out that our simulations favor a value of 105°.

In their recent paper Bockelée-Morvan et al. [2009] indicate that strong compositional inhomogeneities might be present at Hale-Bopp particularly for CO sources. The investigators report about a CO jet at a latitude position of 20° from which 40% of the observed outgassing may originate *from*. Finally, Bockelée-Morvan et al. [2009] also report about the lack of a correlation between the CO jet and dust jets. Earlier, Lederer and Campins [2002] also wrote that comet Hale-Bopp appears to be chemically heterogeneous. These reports gave us a solid observational argument to study CO activity at different latitudes.

3.3. Results for CO activity

The integrated CO activity F_{CO} of Hale-Bopp is compared with observations. Activity is calculated through integration over the whole spherical

ACCEPTED MANUSCRIPT

nucleus

$$F_{CO} = f_a \frac{2\pi}{\tau_r} R^2 \int_0^{\pi} d\theta \sin(\theta) \int_0^{\tau_r} dt\, q_{CO}(\theta, t)\,. \tag{26}$$

$$\mathbf{F_{CO}} = \mathbf{f_a} \frac{\mathbf{2}\pi}{\tau_\mathbf{r}} \mathbf{R^2} \int_{-\pi/\mathbf{2}}^{\pi/\mathbf{2}} \mathbf{d}\theta \cos(\theta) \int_{\mathbf{0}}^{\tau_\mathbf{r}} \mathbf{dt}\, \mathbf{q_{CO}}(\theta, \mathbf{t})\,. \tag{27}$$

R is its radius, under the assumption that the comet is spherically symmetric. The fraction f_a of active surface areas is employed to fit the observations with the calculated production curves.This approach is commonly used although it might not always be stated. q_{CO} denotes the CO flux from a latitude θ at time t at the surface.

For a thermal conductivity of 0.01 W m^{-1} K^{-1} the CO production curve is shown in Fig. 3. It is assumed that the active CO spots are distributed over the whole nucleus. The spherical nucleus is divided in latitudinal direction into stripes with a thickness of 25°. The obliquity of the comet was set to 84° and the argument of the sub-solar meridian Φ had a value of 105°. Apparently, the model is not able to reproduce the CO production rates of Biver et al. [2002]. Only close to perihelion, the model seems to fit the observations.

This result is in agreement with previous reports. So far only Enzian [1999] and Capria et al. [2002] were able to present good fits of the CO observations, however, only over a limited heliocentric distance from -7 to 4 AU. Both groups assumed a certain amount of CO gas trapped in amorphous ice, a certain amount of CO bulk ice to be present, and a certain amount of CO *subliming***sublimating** only when water ice sublimes. The latter mechanism was proposed by Capria et al. [2002]. **A** similar assumption on the existence of amorphous ice was also made in Prialnik [1997a] and Prialnik [1997b].

ACCEPTED MANUSCRIPT

However, there is still no observational evidence for amorphous ice in the Solar System [Huebner , 2009]. Therefore we do not follow the more or less ad hoc assumption of amorphous ice in cometary nuclei. The most straight forward approach has been to assume CO bulk ice sublimation and to perform an integration over the whole nucleus. But this approach has failed [Capria et al., 2000].

Recent observational findings concerning the chemical heterogeneity [Lederer and Campins, 2002; Bockelée-Morvan et al., 2009] and a CO jet at a latitude of 20° [Bockelée-Morvan et al., 2009] indicate that cometary activity might be localized. Therefore, the CO activity of Hale-Bopp at different latitudes is investigated. In Fig. 4, CO activity along the pre-perihelion branch is depicted. This result indicates that confining CO activity on the positive hemisphere above +10° could fit the observations. The CO activity for different latitudinal heights along the post-perihelion branch is depicted in Fig. 5. It is apparent that a very good fit for the post-perihelion CO data of Biver et al. [2002] is obtained if CO activity is confined to the positive hemisphere above +10° as in the pre-perihelion case. The result of such a scenario is displayed in Fig. 6.

The model is able to fit the CO observations of Biver et al. [2002] *remarkably* **very** well over the whole measured heliocentric distance starting at -7AU pre-perihelion to almost 15AU post-perihelion. The fraction of active surface elements f_a was set to 0.75. *The presented CO curve seems to be in a very good agreement with the CO jet at a latitude of 20° as reported by Bockelée-Morvan et al. [2009] for the observations at 11 March 1997, which was close to perihelion on the pre-perihelion branch.***The restriction**

ACCEPTED MANUSCRIPT

to northern hemisphere CO sublimation is consistent with the CO jet at a latitude of 20° as reported by Bockelée-Morvan et al. [2009] for the observations at 11 March 1997, which was close to perihelion on the pre-perihelion branch. At around -2AU pre-perihelion the model approximates the local peak in the observations by a plateau.

3.4. Results for water activity

The water production curve for the best CO scenario of the previous section is depicted in Fig. 7. It is assumed that the positive hemisphere above 10° is active in water and CO while the remaining nucleus surface is still outgassing water vapor but not CO. The model is able to reproduce the general trend of the water observations throughout the orbit. The fraction of active surface elements f_a is about 0.25. This result is in agreement with Kührt [1999]. Our fit of the water observations is slightly better than that presented in Enzian et al. [1998], Enzian [1999], and Capria et al. [2002]. These groups argue that beyond 4AU pre-perihelion water activity could only be due to icy grains in the coma while around perihelion nucleus activity is mainly responsible for the observed water activity of Hale-Bopp. Enzian et al. [1998] gave an estimate of the water activity of icy grains in the coma. The water production curve of *this* **that** estimate seems to fit the water observations beyond 4AU on the pre-perihelion branch. Along the post-perihelion branch, the water production rates, however, could not be reproduced **with the assumption of extended water sources as proposed by Enzian et al. [1998]**.

In a recent article, Lederer et al. [2009] analyzed Hale-Bopp data with a Monte Carlo model which indicates that extended sources due to icy grains in

ACCEPTED MANUSCRIPT

the coma might contribute to water activity. The simulations were performed on data from April 22-26, 1997. At that time the comet was at the beginning of its post-perihelion branch.

Currently, it is difficult to judge to what extend cometary water activity could be due to extended sources and whether these sources contribute significantly to the observed water activity of this comet on its whole orbit or whether it is only a transient effect. **It is also conceivable to achieve better agreement between the model calculations and the observed water activity of Hale-Bopp by fine-tuning the placement of active areas and their size, the spin pole vector, and by abandon the assumed spherical nucleus shape.**

3.5. Results for different values of the argument Φ of the subsolar meridian at perihelion

The illumination of a surface area on the nucleus depends according to Sekanina [1979] on the angle between the equatorial plane of the comet and the orbit plane, e.g. obliquity of the comet, and the argument Φ of the subsolar meridian at perihelion. These values enter the calculation of the solar zenith angle ζ according to Eq. (13) and Eq. (14). Unfortunately, these values are not so well constrained but they clearly influence the outgassing pattern of the nucleus.

This should briefly be demonstrated for CO. The CO production curve for the best fit scenario of Section 3.3 is shown in Fig. 8 for an argument Φ of 105° and 95°. Thus, changing Φ by a value of 10° shifts the CO outgassing curve clearly. Hence, this parameter must be treated carefully when comparing simulations with observations.

ACCEPTED MANUSCRIPT

4. Discussion and conclusions

A *novel* thermophysical approach is presented to interpret the observations of comet Hale-Bopp as reported by Biver et al. [2002].

The nucleus model accounts for heat conduction, heat advection, gas diffusion, sublimation, and condensation in an ice-dust matrix with moving boundaries. Surface erosion due to surface sublimation leads to a moving boundary which is resolved by applying a temperature remapping technique. This approach allows to take properly into account the loss in the internal energy of the eroded surface layers. Such moving boundary techniques are referred to as Stefan problems.

Our approach is guided by recent observational findings on important parameters controlling cometary activity. A low thermal conductivity [Kührt , 1999; Groussin et al., 2007], the obliquity of the rotation axis [Jorda et al., 1997], the chemical heterogeneity [Lederer and Campins, 2002; Bockelée-Morvan et al., 2009], and the CO jet at a latitude of 20° [Bockelée-Morvan et al., 2009] have been incorporated to calculate the water and CO activity.

For the first time, a thermal model is applied to the full data set of the water and CO production rates as reported by Biver et al. [2002]. The data set covers the heliocentric range from -7AU pre- to 15AU post-perihelion. *There was no need to include amorphous ice into the model.* The following results were obtained:

- *The measured water production rates are well reproduced by the model.***The model is able to reproduce the water activity from -4 AU pre- to the outgoing leg while it does not describe well the water activity beyond -4 AU.** It is assumed that the active spots are

ACCEPTED MANUSCRIPT

distributed randomly over the whole nucleus.

- The CO production curve fits the observations over the whole heliocentric distance starting at -7AU to 15AU *very well. In agreement*Consistent with recent reports by Bockelée-Morvan et al. [2009] about a CO source at a latitude of 20° the best fit to the observations was obtained if CO activity is confined to the positive hemisphere above a latitude of 10°. Around -2AU pre-perihelion, the model approximates the local peak of the CO observations by a plateau. *The CO fit along the post-perihelion branch is astonishingly well.*

- A low thermal conductivity of 0.01 W $K^{-1}m^{-1}$ is in good agreement with the Hale-Bopp observations.

In conclusion, currently there are two distinctly different approaches to model the outgassing pattern of Hale-Bopp for water and CO as reported by Biver et al. [2002]. The approaches of Enzian [1999], Capria et al. [2002], and Prialnik [1997b] on the one hand. These models rely on the assumption that some form of amorphous ice must be present in the comet, that a certain percentage of CO must be trapped in the amorphous ice matrix which is released after phase transition, and that there is a certain percentage of CO bulk ice. On the other hand, the approach of this paper which tries to incorporate as many observational findings of the recent years as possible and which relies only on CO bulk **ice**.

Finally, the importance of the argument Φ of the sub-solar meridian at perihelion for the CO production curve has also been demonstrated. The argument Φ and the obliquity of the comet determine the distribution of the

ACCEPTED MANUSCRIPT

incoming solar energy on the nucleus surface. Changing Φ by a value of 10° shifts the CO production curve clearly.

ACCEPTED MANUSCRIPT

ACCEPTED MANUSCRIPT

5. Acknowledgements

We thank Detlef de Niem for discussions on the Stefan Problem. We are very grateful to B. Davidsson and H. Rickman for discussions on the thermal physics of comets. One of us (E. K.) would like to thank Prof. J. Geiss for fruitful discussions during a stay at the International Space Science Institute (ISSI) in Bern. **We appreciate the valuable comments of B. Davidsson and an anonymous referee who helped to improve the paper.**

ACCEPTED MANUSCRIPT

ACCEPTED MANUSCRIPT

6. Plots

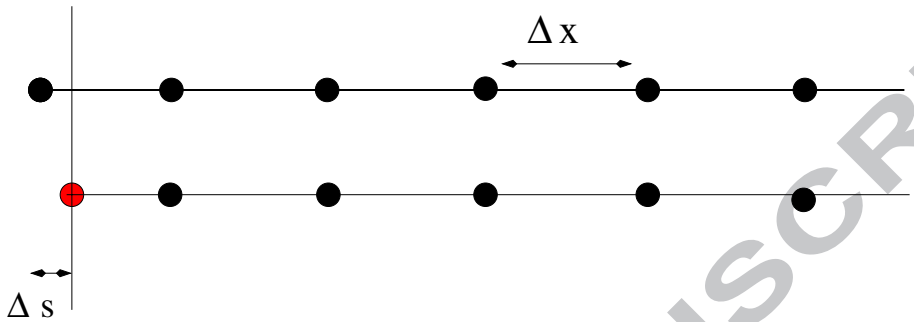

Figure 1: Due to surface sublimation a certain amount of material is ejected from the surface of the nucleus. This leads to a moving boundary and to a deviation between the actual grid and the current position of the surface. Special techniques are necessary for a proper treatment.

ACCEPTED MANUSCRIPT

ACCEPTED MANUSCRIPT

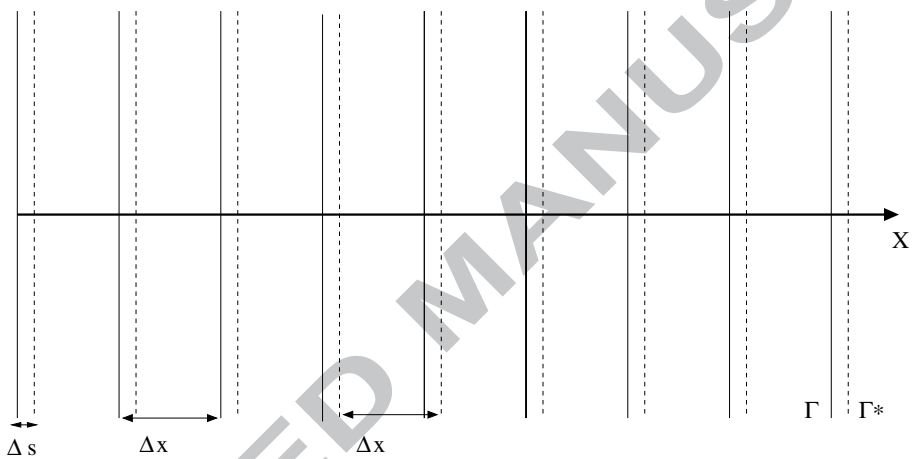

Figure 2: The spatial discretization size Δx remains constant throughout the computation. The old grid Γ is moved according to the erosion of surface material Δs. The temperature field at the new grid Γ^* is obtained through interpolation with cubic splines [Crank and Gupta , 1972].

ACCEPTED MANUSCRIPT

ACCEPTED MANUSCRIPT

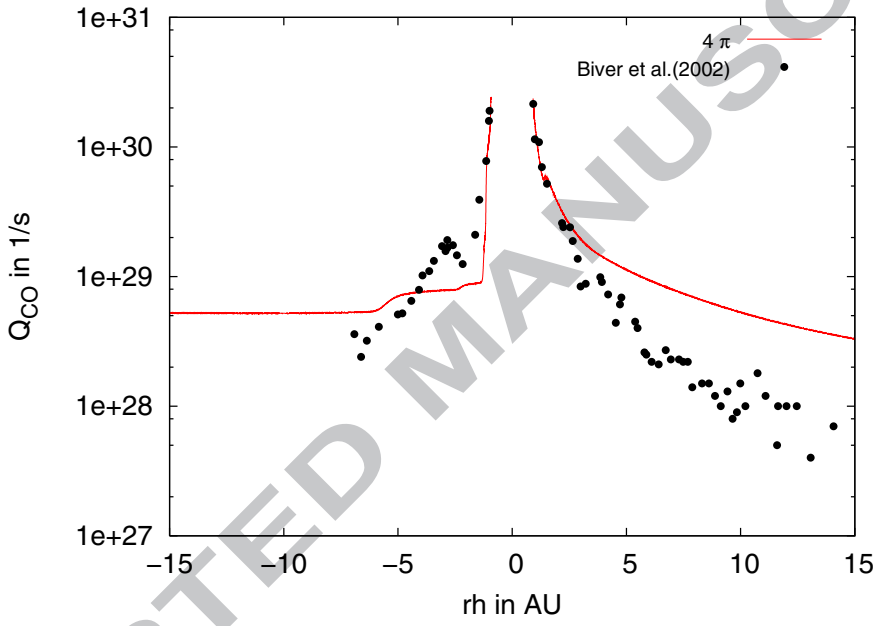

Figure 3: CO production curve plotted as function of heliocentric distance. The curve is calculated by integration over the whole spherical nucleus. The fraction of active surface elements was about 0.25. The CO curve fits the CO data of Biver et al. [2002] only close to perihelion well.

ACCEPTED MANUSCRIPT

ACCEPTED MANUSCRIPT

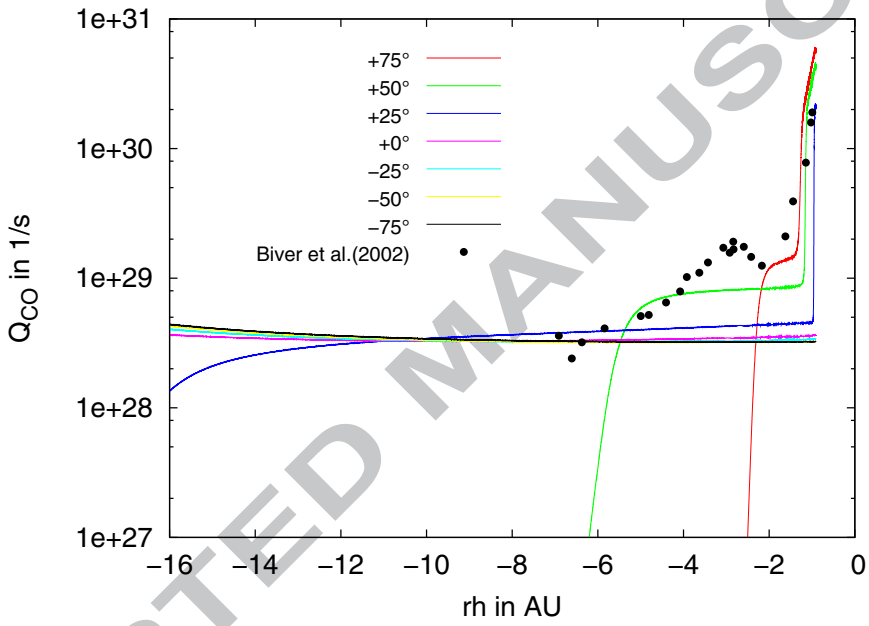

Figure 4: Similar CO plot as in Fig. 3. The CO production of seven latitudinal stripes with thickness of 25° are presented along the pre-perihelion branch. The CO data of Biver et al. [2002] could be fitted if CO activity is confined to the positive hemisphere above a latitude of +10°.

ACCEPTED MANUSCRIPT

ACCEPTED MANUSCRIPT

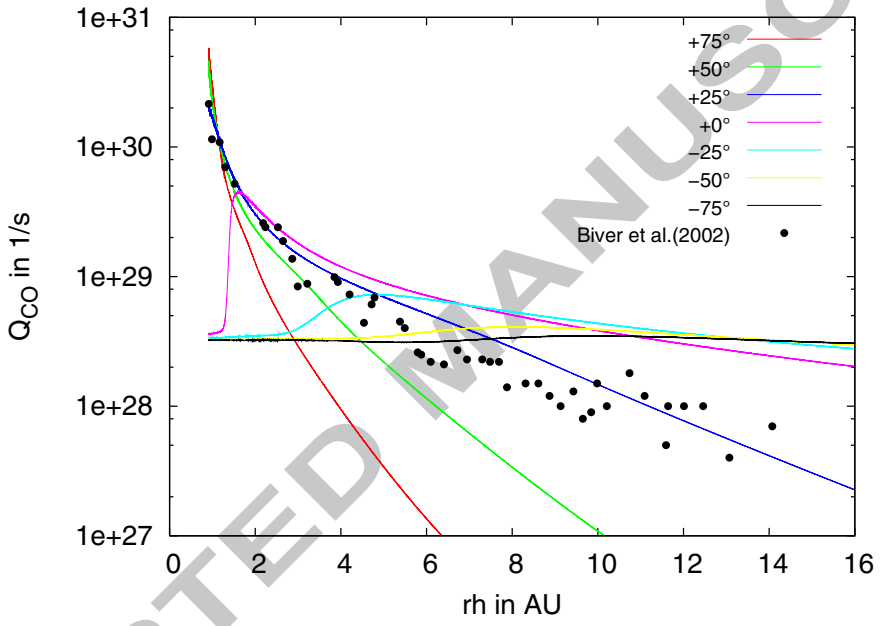

Figure 5: Similar CO plot as in Fig. 4 for the post-perihelion branch. The CO data of Biver et al. [2002] along the post-perihelion branch could be fitted if CO activity is confined to the positive hemisphere above a latitude of +10° as in the pre-perihelion case of Fig. 4.

ACCEPTED MANUSCRIPT

ACCEPTED MANUSCRIPT

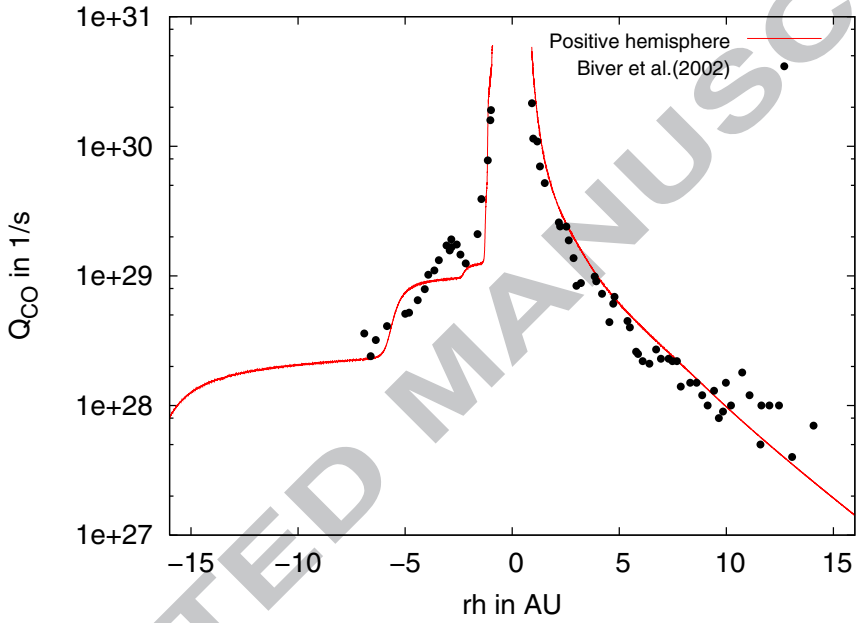

Figure 6: Similar CO plot as in Fig. 3. The CO production curve is integrated over the positive hemisphere above 10°. The fraction of active surface elements was 0.75. The CO data of Biver et al. [2002] are well reproduced along the pre-perihelion branch and remarkably well along the whole post-perihelion branch covering a heliocentric distance from 1AU to almost 15AU. The local peak at around -2AU is approximated by a plateau.

ACCEPTED MANUSCRIPT

ACCEPTED MANUSCRIPT

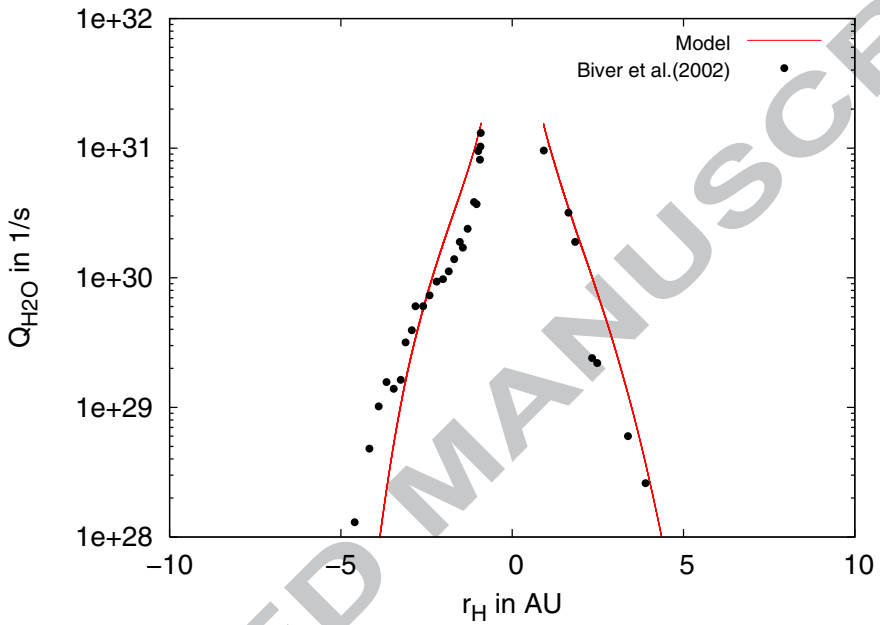

Figure 7: Water production curve of Hale-Bopp plotted as function of heliocentric distance. The production curve is obtained through integration over a spherical nucleus with a fraction of active surface elements of 0.25. CO activity takes place on the positive hemisphere above 10° according to the best fit scenario of Fig. 6 while water active surface areas are distributed over the whole nucleus. *The general trend of the water production rates of Biver et al. [2002] are reproduced over the whole range.***Beyond -4 AU pre-perihelion the model is not able to reproduce well the water activity. From -4AU to the outgoing leg water activity is well reproduce. This can be even improved if the fraction of active surface elements is reduced.**

ACCEPTED MANUSCRIPT

ACCEPTED MANUSCRIPT

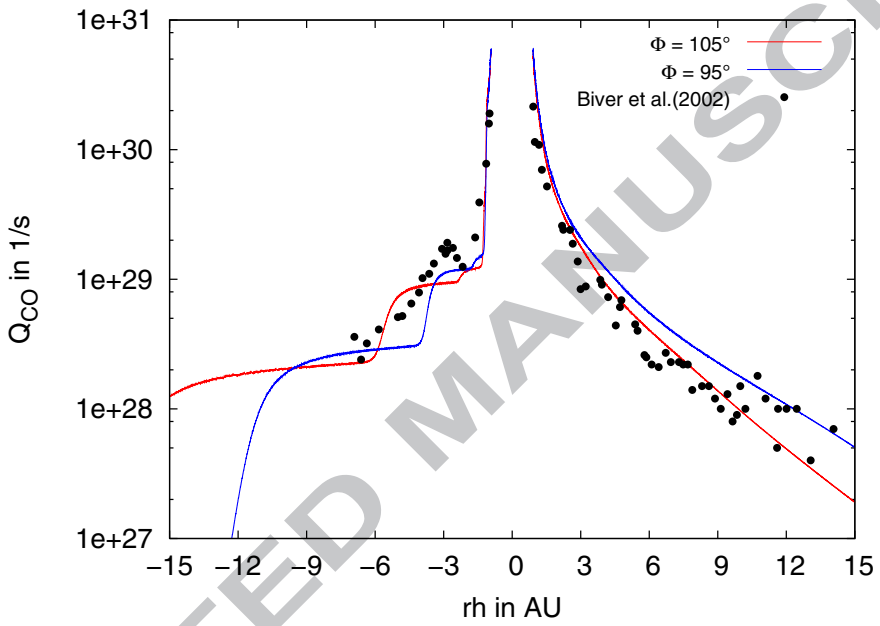

Figure 8: Similar CO plot as in Fig. 6. The importance of the argument of the sub-solar meridian at perihelion Φ for the CO production curve is demonstrated. Changing the argument by 10° shifts the outgassing curve, because the illumination conditions of the different latitudes throughout the orbit change. The obliquity was throughout this paper 84°. The argument Φ and the obliquity enter the calculation of the solar zenith angle ζ [Sekanina , 1979].

ACCEPTED MANUSCRIPT

ACCEPTED MANUSCRIPT

7. Tables

Table 1: Basic parameters.

Quantity	Symbol	Value
Density of water ice	ρ_i	917 kg/m^3
Specific heat of water ice	c_i	1610 J/(kg K)
Specific heat of water gas	$c_{g,i}$	1370 J/(kg K)
Pressure constant water ice	A_i	3.56×10^{12} Pa
Temperature constant water ice	B_i	6141.667 K
Thermal enthalpy of water ice	ΔH_i	2.84×10^6 J/kg
Density of CO ice	ρ_{co}	1250 kg/m^3
Specific heat of CO ice	c_{co}	2010 J/(kg K)
Specific heat of CO gas	$c_{g,co}$	720 J/(kg K)
Pressure constant CO ice	A_{co}	1.2361×10^9 Pa
Temperature constant CO ice	B_{co}	764.16 K
Thermal enthalpy of CO ice	ΔH_{co}	0.227×10^6 J/kg
Density of dust	ρ_d	3000 kg/m^3
Specific heat of dust	c_d	1300 J/(kgK)
Emissivity	ϵ_{em}	0.96
Bond Albedo	$\mathcal{A}$	0.04

ACCEPTED MANUSCRIPT

ACCEPTED MANUSCRIPT

Table 2: Set of model parameters.

Quantity	Symbol	Value
Mass concentration of water ice	X_i	0.4
Mass concentration of CO ice	X_{co}	0.1
Mass concentration of dust	X_d	0.5
Porosity	ψ	0.5
Pore radius	r_p	100μm

Table 3: Orbital and rotational parameters of Hale-Bopp. JPL denotes the NASA Small-Body Database.

Quantity	Symbol	Value	Source
Eccentricity	ϵ	0.9950817161	JPL
Semi-major axis	a_{semi}	185.864AU	JPL
Diurnal rotation period	τ_r	11.4 h	Jorda et al. [1997]
Orbital rotation period	t_{orb}	2500 y	JPL
Obliquity of the rotation axis	δ	84 °	Jorda et al. [1997]
Argument of subsolar meridian	Ω	105°	
Nucleus radius	R	30 km	Fernández [2002]

Table 4: Numerical parameters.

Quantity	Symbol	Value
Temporal discretization	Δt	200s
Spatial discretization	Δx	1 mm
Depth of lower boundary	x_b	5 m
Initial depth of the CO front	x_{CO}	50 cm

ACCEPTED MANUSCRIPT

References

Benkhoff, J., Spohn, T., 1991. Results of a coupled heat and mass transfer model applied to KOSI sublimation experiments. In: Kömle, N.,I., Bauer,S. J., Spohn, T.(Eds), Theoretical Modelling of Comet Simulation Experiments. Verlag der Österreichischen Akademie der Wissenschaften, Wien, 31-47.

Biver, N., Bockelée-Morvan, D., Colom, P., Crovisier, J., Germain, B., Lellouch, E., Davies, J. K., Dent, W. R. F., Moreno, R., Paubert, G., Wink, J., Despois, D., Lis, D. C., Mehringer, D., Benford, D., Gardner, M., Phillips, T. G., Gunnarsson, M., Rickman, H., Winnberg, A., Bergman, P., Johansson, L. E. B., Rauer, H., 1997. Long-term evolution of the outgassing of comet Hale-Bopp from radio observations. Earth Moon and Planets 78, 5-11.

Biver, N., Bockelée-Morvan, D., Colom, P., Crovisier, J., Henry, F., Lellouch, E., Winnberg, A., Johansson, L. E. B., Gunnarsson, M., Rickman, H., Rantakyrö, F., Davies, J. K., Dent, W. R. F., Paubert, G., Moreno, R., Wink, J., Despois, D., Benford, D. J., Gardner, M., Lis, D. C., Mehringer, D., Phillips, T. G., Rauer, H., 2002. The 1995-2002 long-term monitoring of comet C/1995 O1 (Hale-Bopp) at radio wavelength. Earth Moon and Planets 90, 5-14.

Bockelée-Morvan, D., Rickman, H., 1997. C/1995 O1 (Hale-Bopp): Gas production curves and their interpretation. Earth Moon and Planets 79, 55-77.

Bockelée-Morvan, D., Henry, F., Biver, N., Boissier, J., Colom, P., Crovisier,

ACCEPTED MANUSCRIPT

J., Despois, D., Moreno, R., Wink, J., 2009. Interferometric imaging of carbon monoxide in comet C/1995 O1 (Hale-Bopp): evidence of a strong rotating jet. Astronom. & Astrophys. 505, 825-843.

Capria, M. T., Coradini, A., De Sanctis, M. C., Blecka, M. I., 2001. P/Wirtanen thermal evolution: effects due to the presence of an organic component in the refractory material, Capria, M. T., Coradini, A., De Sanctis, M. C., Orosei, R., 2000. CO emission mechanisms in C/1995 O1 (Hale-Bopp). Astronom. & Astrophys. 357, 359-366.

Capria, M. T., Coradini, A., De Sanctis, M. C., 2002. C/1995 O1 Hale-Bopp: Short and long distance activity from a theoretical model. Earth Moon and Planets 90, 217-225.

Colom, P., Gérard, E., Crovisier, J., Bockel-Morvan, D., Biver, N., Rauer H., 1997. Observations of the OH radical in Comet HaleBopp with the Nancay Radio Telescope. Earth Moon and Planets 78, 37-43.

Crank, J., Gupta, R. S., 1972. A method for solving moving boundary problems in heat flow using cubic splines or polynomials. J. Inst. Maths Appl. 10, 296-304.

Crank, J., 1984. Free and moving boundary problems. Oxford University Press, New York.

Crovisier, J., Leech, K., Bockelée-Morvan, D., Lellouch, E., Brooke, T. Y., Hanner, M. S., Altieri, B., Keller, H. U., Lim, T., 1999.The Spectrum of Comet Hale-Bopp as seen by ISO. In: Cox, P., Kessler, M. (Eds.), The Universe as Seen by ISO. ESA Special Publication, 137-140.

ACCEPTED MANUSCRIPT

Davidsson, B. J. R., Skorov, Y. V., 2002b. On the Light-Absorbing Surface Layer of Cometary Nuclei II. Thermal Modeling. Icarus 159, 239-258.

Davidsson, B. J. R., Skorov, Y. V., 2004. A practical tool for simulating the presence of gas comae in thermophysical modeling of cometary nuclei. Icarus 168, 163-185.

Davidsson, B. J. R., Gutiérrez, P. J., Rickman, H., 2009. Physical properties of morphological units on Comet 9P/Tempel 1 derived from near-IR Deep Impact spectra. Icarus 201, 335-357.

Enzian, A., Cabot, H., Klinger, J., 1998. Simulation of the water and carbon monoxide production rates of comet Hale-Bopp using a quasi 3-D nucleus model. Planet. Space Sci. 46, 851-858.

Enzian, A., 1999. On the Prediction of CO Outgassing from Comets Hale-Bopp and Wirtanen. Space Science Reviews 90, 131-139.

Fanale, F. P., Salvail, J. R., 1984. An idealized short-period comet model - Surface insolation, H2O flux, dust flux, and mantle evolution. Icarus 60, 476-511.

Fernández, Y. R., 2002. The Nucleus of Comet Hale-Bopp (C/1995 O1): Size and Activity. Earth Moon and Planets 89, 3-25.

Festou, M. C., Keller, H. U., Weaver, H. A., 2004. A brief conceptual history of cometary science. In: Festou, M. C., Keller, H. U., Weaver, H. A. (Eds.), Comets II. Univ. of Arizona Press, Tucson, 3-16.

ACCEPTED MANUSCRIPT

ACCEPTED MANUSCRIPT

Flammer, K. R., Mendis, D. A., Houpis, H. L. F., 1999. On the Outgassing Profile of Comet Hale-Bopp. The Astrophys. J. 494, 822-827.

Groussin, O., A'Hearn, M. F., Li, J.-Y., Thomas, P. C., Sunshine, J. M., Lisse, C. M., Meech, K. J., Farnham, T. L., Feaga, L. M., Delamere, W. A., 2007. Surface temperature of the nucleus of Comet 9P/Tempel 1. Icarus 187, 16-25.

Grün, E., Gebhard, J., Bar-Nun, A., Benkhoff, J., Dueren, H., Eich, G., Hische, R., Huebner, W. F., Keller, H. U., Klees, G., 1993. Development of a dust mantle on the surface of an insolated ice-dust mixture - Results from the KOSI-9 experiment. J. Geophys. Res. 98, 15091-15104.

Huebner, W. F., 2009. Origins of Cometary Materials, In: Balsiger, H., Altwegg, K., Huebner, W., Owen, T., Schulz, R (Eds.), Origin and Early Evolution of Comet Nuclei, The International Space Science Institute, Bern, Switzerland, 5-25.

Jewitt, D., Senay, M., Matthews, H., 1996. Observations of Carbon Monoxide in Comet Hale-Bopp. Science 271, 1110-1113.

Jorda, L., Rembor, K., Lecacheux, J., Colom, P., Colas, F., Frappa, E., Lara, L. M., 1997. The Rotational Parameters Of HaleBopp (C/1995 O1) From observations of the dust jets at Pic du Midi observatory. Earth Moon and Planets 77, 167-180.

Lederer S. M., Campins, H., 2002. Evidence for Chemical Heterogeneity in the Nucleus of C/1995 O1 (Hale-Bopp). Earth Moon and Planets 90, 381-389.

ACCEPTED MANUSCRIPT

Lederer S. M., Campins, H., Osip D. J., 2009. Chemical and physical properties of gas jets in comets: II. Modeling OH, CN and C2 jets in Comet C/1995 O1 (HaleBopp) one month after perihelion. Icarus 199, 484-504.

Kührt, E., 1999. H2O-Activity of Comet Hale-Bopp. Space Science Reviews 90, 75-82.

Mekler, Y., Prialnik, D., Podolak, M., 1990. Evaporation from a porous cometary nucleus, The Astrophys. J. 356, 682-686.

Prialnik, D., 1997a. A Model for the Distant Activity of Comet Hale-Bopp. Astrophys. J. Lett. 478, 107-110.

Prialnik, D., 1997b. Modelling Gas and Dust Release from Comet Hale-Bopp. Earth Moon and Planets 77, 223-230.

Seiferlin, K., 1991. The thermal conductivity of porous ice with application to KOSI sample material: A review. In: Kömle, N. I., Bauer, S. J., Spohn, T. (Eds.), Theoretical Modelling of Comet Simulation Experiments, Verlag der Österreichischen Akademie der Wissenschaft, 49-66.

Seiferlin, K., Kömle, N. I., Kargl, G., Spohn, T., 1996. Line heat-source measurements of the thermal conductivity of porous H_2O ice, CO_2 ice and mineral powders under space conditions. Planet. Space Sci. 44,691-704.

Sekanina, Z., 1979. Fan-shaped coma, orientation of rotation axis, and surface structure of a cometary nucleus. I - Test of a model on four comets . Icarus 37, 420-442.

ACCEPTED MANUSCRIPT

Skorov, Y. V., Kömle, N. I., Keller, H. U., Kargl, G., Markiewicz, W. J., 2001. A Model of Heat and Mass Transfer in a Porous Cometary Nucleus Based on a Kinetic Treatment of Mass Flow. Icarus 153, 180-196.

Spohn, T., Benkhoff, J., Klinger, J., Grün, E., Kochan, H., 1989. Thermal modelling of two KOSI comet nucleus simulation experiments. Adv, Space Sci. 9, 127-131.

Spohn, T., Benkhoff, J., 1990. Thermal history models for KOSI sublimation experiments. Icarus 87, 358-371.

Stefan, J., 1891. Über die Theorie der Eisbildung, insbesondere über die Eisbildung im Polarmeere. Ann. der Phys. und Chem. 42, 269-286.

Steiner, G., Kömle, N. I., 1991. Thermal budget of multicomponent porous ices. J. Geophys. Res. 96, 18897-18902.

Stern, S. A., Colwell, W. B., Festou, M. C., Tamblyn, P. M., Parker, J. W., Slater, D. C., Weissman, P. R., Paxton, L. J., 1999. Comet Hale-Bopp (C/1995 O1) Near 2.3 AU Postperihelion: Southwest ultraviolet imaging system measurements of the H_2O and dust production. Astrophys. J. 118, 1120-1125.

Stöffler, D., Duren, H., Knolker, J., Hische, R., Bischoff, A., 1991. Cometary analogue material - Preparation, composition, and thin section petrography. Geophys. Res. Lett. 18, 285-288.

Vasundhara, R., Chakraborty, P., 1999. Modeling of Jets from Comet Hale-Bopp (C/1995 O1): Observations from the Vainu Bappu Observatory. Icarus 140, 221-230.

ACCEPTED MANUSCRIPT

Weaver, H. A., Feldman, P. D., A'Hearn, M. F., Arpigny, C., Brandt, J. C., Stern, S. A., 1999. Post-Perihelion HST Observations of Comet Hale-Bopp (C/1995 O1). Icarus 141, 1-12.

ACCEPTED MANUSCRIPT

ACCEPTED MANUSCRIPT

- The CO and water activity of comet C/1995 O1 (Hale-Bopp) is simulated.
- Erosion due to surface sublimation of water ice is treated as a Stefan Problem.
- The CO production curve is a good fit to the measurements over the whole range.
- The best fit of the data is obtained with a thermal conductivity of 0.01 W/(mK).

ACCEPTED MANUSCRIPT